Simulation for thermomechanical behaviour for Shape Memory Alloys (SMA) connection rings of Ultra-High Vacuum (UHV) chambers

Gurrì Simona[1,2], Cardile Federico[1,2], Feugueur Gérald[1], Belhadj Chiraz[3]

[1] Département Mécanique, EPF École d'Ingénieur-e-s, Sceaux, France
[2] DIMEAS Dipartimento Di Ingegneria Meccanica e Aerospaziale, Politecnico di Torino, Torino, Italy
[3] MINES Paristech, PSL Research University, Centre des Matériaux, Évry, France

E-mail:
simona.gurri@studenti.polito.it,
federico.cardile@studenti.polito.it,
gerald.feugueur@epfedu.fr,
chiraz.belhadj@mines-paristech.fr

16 January 2020

Abstract

This paper presents a numerical simulation of the Shape Memory Alloys (SMA) behaviour used for connection rings of Ultra-High Vacuum (UHV) chambers. These materials provide an easy, compact, leak tight and easily mountable/dismountable connection system by applying a simple thermomechanical cycle and they also offer the possibility to connect pipes made of different materials.
Phase transformation can be induced either by stress or temperature changes. These materials take advantage of the shape memory effect of NiTi rings, that consist in the possibility to recover a precise shape by applying a thermal cycle activating the phase change effect, that creates a strong leak tight coupling.
SMA rings will be simulated in 2D firstly with a weak thermo-mechanical coupling then with a strong thermo-mechanical coupling and finally the phase change phenomena will be added. Finite elements analysis (FEM) to visualize temperatures and stresses in the ring will be adopted by using Python. The mounting cycle will be simulated, and real values for both stresses and temperature will be obtained.
The work is focused over the peculiar behavior of SMA rings and to satisfy the functioning request in terms of pressure to avoid any leak. The objective is to have a easy tool to simulate numerically SMA alloys to push over the development of such technologies.

Keywords: Shape Memory effect (SME), phase changing, NiTi alloys, Ultra-High Vacuum (UHV) chambers, Finite Elements Analysis (FEM)

1. Introduction

Context

Smart Materials are receiving big attention in recent years for their great potential to revolutionize the engineering of actuation and control. Shape Memory Alloys (SMAs) are one such 'smart material' that is currently being studied with great enthusiasm as they hold the promise for many engineering advancements in the near future. They are capable of recovering very large strains due to crystallographic transformations between the highly symmetric parent phase of austenite and low symmetry product phase of martensite. These materials have several applications, but are mainly used for particle accelerators, gravitational wave detectors, atomic physics, microscopy (e.g. atomic force and scanning

tunneling) and biomedical applications (Stents). We will analyze an Ultra High Vacuum chamber (UHV) that is a chamber working at a particle density really below the atmospheric one (regimes of pressures are between 10^{-7} and 100 nanopascals), so seals and gaskets used in a UHV system must prevent every trace leakage. The materials used in UHV condition need to stand heating at more than 393°K for many hours per day but also shouldn't present high vapor pressure. So, it is not possible to use plastics, PTFE, PEEK neither glue (screws are used instead), lead (soldering). This is the reason why UHV chamber are more expensive than conventional vacuum ones. Moreover, a baking process is used to remove gas atoms from the chamber wall surfaces. To respect all these constraints SMA alloys, such as NiTinol , are used to join toghether UHV pipes as they provide an easy, compact, leak tight and easily mountable/dismountable connection system [1].

The peculiaruty of SMAs alloys is the pseudo-elasticity (PE) [2] that corresponds to the ability of the material to elongate in large proportion (up to 8%) under tensile loading and to recover to its prior shape when unloaded. Pseudo-elasticity is caused by solid state phase transition between the body-centered cubic austenitic structure austenitic (A) and the monoclinic martensitic one (M), transformation that leads to a distortion of the crystal lattice, that causes the increase of strain. The phase transition is associated with heat emission (or absorption during a reverse loading). Since the phase transformation is induced either by temperature or stress, the local temperature fluctuations strongly change the rate of transformation bands. Associated with low strengthening, localisation usually occurs leading to so-called ‘‘transformation bands’’.

The phase transition is activated either by temperature variation (TIM, Thermally-Induced Martensite) or by applied stress (SIM, Stress-Induced Martensite). SMA-based couplers can be activated remotely, i.e. mounting and dismounting operations can be performed by temperature variations between the Transformation Temperatures (TTs) of the alloy. It represents a relevant advantage especially for applications in radioactive areas of particle accelerators by the fact that mounting operations can be performed remotely by heating the junction unit and so the radiation doses absorbed by the operators could be significantly reduced. [3]

Phase change in SMA also depends on the stress applied, in figure 2 it is possible to see the tensile test effectuated over an SMA alloy sample and it is possible to appreciate the change in Young modulus E according to the stress applied. [4]

Contact analysis will be made with a multi-physical coupling, in which the pipe will be considered as an infinite rigid body while the ring is deformed in the plane stress 2D hypothesis by means of the temperature and phase changing. At each time step, the results in term of temperature and stress will be given and compared with the minimum pressure value.

The problem will be modeled by means of Phython with Finite Elements Method (FEM) for the space resolution, whilst Finite Differences with an implicit scheme will be used to discretize the evolution in time.

The aim is to provide a reliable and fast tool to simulate numerically the behavior of SMA alloys to push over the development of such innovative technologies.

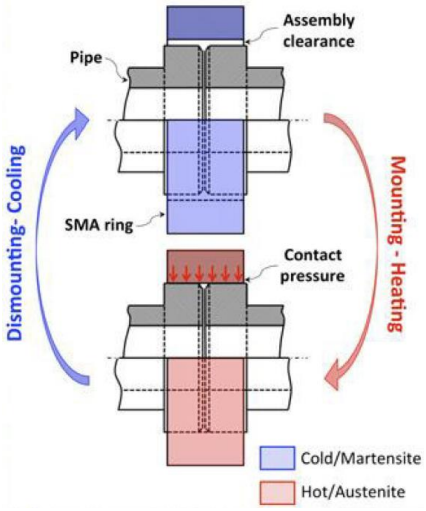

Figure 1 - Functioning principle of the ring [3]

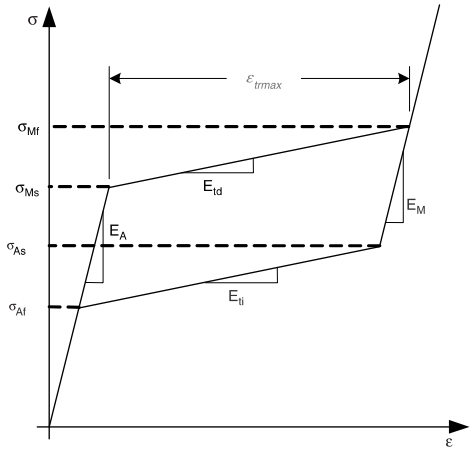

Figure 2-Engineering stress-strain curve for SMA alloys [6]

2. Literature review

2.1 Functioning principle/cycle

Beam-pipe couplings are generally guaranteed by means of detachable connections systems. Austenitic stainless steels are widely used for vacuum chambers and coupling flanges because they fulfil most of the stringent requirements for UHV and are easily obtainable at a reasonable cost. Dismountable seals and valves are mainly made of stainless steels used in conjunction with softer metal gaskets (i.e. aluminium or copper) which allow high baking temperatures (above 573°K) and create leak-free metal joints. The gasket seals are defined

as deformable and resilient parts placed between two rigid surfaces, the flanges, to obtain a leak-free seal. The seals form leak-tight joints loaded by compressing a gasket between the sealing parts.

Expanded cooled SMA ring has an inner diameter that is larger than vacuum's chamber outside diameter, by heating it up it shrinks onto the vacuum chamber assuring its leak tightness at room temperature. Normally, the mounting cycle of the SMA is made as follows [2]:

• Mechanical pre-strain in martensitic condition ($T<M_f$) (figure 2, point 1)

•Mounting with clearance between ring and pipe (figure 2, point 2)

• Thermal activation (SME) at $T=A_s$ (figure 2, point 3.1)

• SMA-ring pipe contact (figure 2, point 3.2)

• Complete activation ($T=A_f$) (figure 2, point 3.3)

• Cooling down to T_{op} (figure 2, point 3.4)

A_S	A_F	M_S	M_F
313 K	323 K	248 K	223 K

Table 1-Temperatures of phase change for NiTi

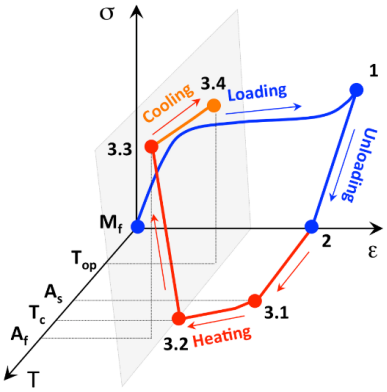

Figure 3 - Mounting Cycle [1]

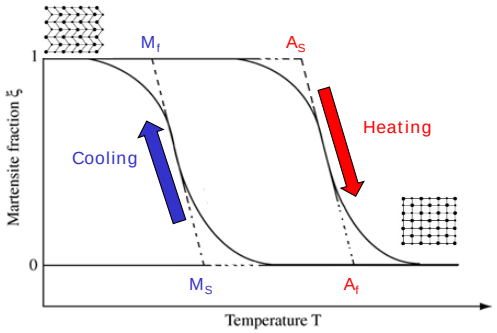

Figure 4- Percentage of Martensite as function of T [1]

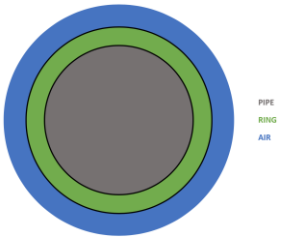

Figure 5 - Model of the system

Considering the problem axial symmetric, a 1D analysis trough the radius will be done. Behaviour laws are presented considering a plane stress hypothesis due to low thickness of the ring. From the thermal point of view, the temperature in each section is homogeneous and thermal gradients in transverse directions will be neglected.

2.2 Properties

It is possible to summarize the geometrical parameters and the property of SMA ring [5] as follows:

Density ρ	6500 kg/m^3
Thermal conductivity λ	$1.8 \cdot 10^{-2}$ W/mmK
Poisson ratio ν	0,33
Specific heat capacity c_P	322 J/kgK

Table 2- Material properties

Property	Martensite	Austenite
Young Modulus E	28000 MPa	75000 MPa
Yield strength R_{P02}	150 MPa	650 MPa
Coefficient of thermal expansion α	$6{,}6 \cdot 10^{-6}$ $/°K$	$11 \cdot 10^{-6}$ $/°K$

Table 3-NiTi phases' properties

$D_{e\,air}$	$D_{i\,air}=D_{e\,SMA}$	$D_{i\,SMA}$
$100\ mm$	$60mm$	$44mm$

Table 4-Diameters of the SMA ring and the air

2.3 Behaviour Laws

To approach the problem, a partition of the strain in elastic strain ε_{el}, thermal strain ε_{th}, and transformation strain due to phase change ε_{tr} has been used:

$$\varepsilon(r,t) = \varepsilon_{el}(r,t) + \varepsilon_{th}(r,t) + \varepsilon_{\phi}(r,t) \quad (2.1)$$

Elastic strain is the strain due to elastic stress, that obeys to Hooke's law: $\varepsilon_{el}(r,t) = \frac{\sigma(T)}{E(r,t)}$ (2.2)

Thermal strain is the strain due to the thermal expansion given by a change in temperature defined as:

$$\varepsilon_{th}(r,t) = \alpha(T(r,t) - T_{air}) \quad (2.3)$$

For the stress variation due to phase change, a modelling depending on temperature has been done. In the temperature range in which austenite starts to be formed (A_s) and ends his formation (A_f) a residual strain due to phase changing appears. It gets two possible values, zero if the matter remains austenitic or $\varepsilon_{\phi max}$ when the maximum transformation strain if the matter becomes martensitic ($\varepsilon_{\phi max}=\varepsilon_{\phi aust}=0{,}001$). To better simulate the behaviour between $T=A_s$ and at $T=A_f$, a probability law has been adopted as follows:

$$\varepsilon_{\phi}(T) = \varepsilon_{\phi_{mart}} \overline{\Psi}_{\mu,\sigma}(T) + \varepsilon_{\phi_{aust}} \Psi_{\mu,\sigma}(T) \quad (2.4)$$

With: $\overline{\Psi}_{\mu,\sigma}(T) = 1 - \Psi_{\mu,\sigma}(T)$

And: $\Psi_{\mu,\sigma}(T) = \frac{1}{\sigma\sqrt{2\pi}} \int_{-\infty}^{T} e^{-\frac{1}{2}\left(\frac{x-\mu}{\sigma}\right)^2} dx$

Where μ is the average temperature between A_s and A_f (318 K); Ψ is the chosen function of austenite as a function of temperature; $\sigma^2 = 0{,}366$ is the variance of the normal distribution considered.

The same approach has been used to take into account of the variation of Young modulus (E) and the coefficient of thermal expansion (α) in the temperature range between A_s and A_f:

$$E(T) = E_{mart} \overline{\Psi}_{\mu,\sigma}(T) + E_{aust} \Psi_{\mu,\sigma}(T) \quad (2.5)$$

$$\alpha(T) = \alpha_{mart} \overline{\Psi}_{\mu,\sigma}(T) + \alpha_{aust} \Psi_{\mu,\sigma}(T) \quad (2.6)$$

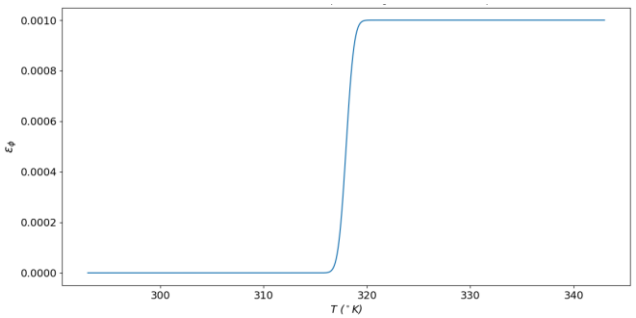

Figure 6-Strain due to phase change as a function of temperature

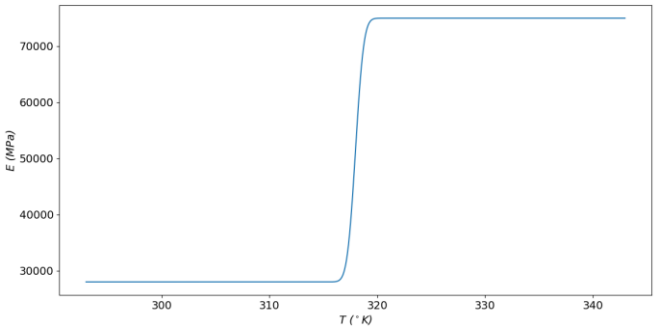

Figure 7-Young Modulus as a function of temperature

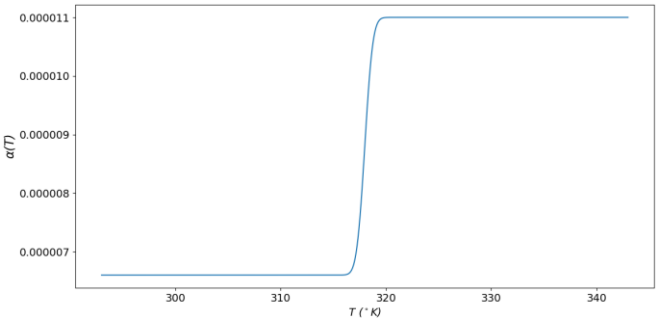

Figure 8-Coefficient of thermal expansion as a function of temperature

To pass to the expression of stress, for isotropic elastic materials the stress-strain relation holds:

$$\underline{\sigma}(r,t) = 2\mu\underline{\varepsilon} + \lambda\, tr(\underline{\varepsilon}) \cdot \underline{I} \quad (2.7)$$

With: $\mu = \frac{E}{2(1+\nu)}$ and $\lambda = \frac{\nu E}{(1+\nu)(1-2\nu)}$

That for a 1D case is reduced as follow:

$$\underline{\sigma}(r,t) = 2\mu\underline{\varepsilon} + \lambda\,\underline{\varepsilon} \quad (2.8)$$

Exploiting the expression of the strains, we lead to a final formulation as follows:

$$\sigma = (2\mu + \lambda)\varepsilon_{el} + (2\mu + \lambda)\alpha\Delta T \quad (2.9)$$

In the weak coupling the strain variation due to change in temperature will be calculated at each time step to find out the stress level at each node.

In the strong coupling, the fact that there is a variation of stress that provokes a further variation of temperature is considered at each time step.

The phase changing is considered at each time step by including the strain ε_ϕ in the stress-strain equation.

For sake of clarity, a scheme of the complete coupling is here proposed:

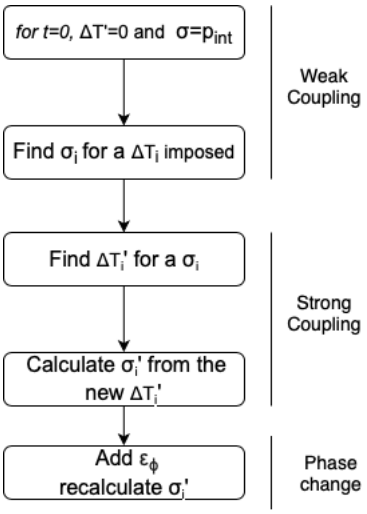

Figure 9 - Scheme of the calculation procedure

3. Modelling

3.1 Numerical Methods

As shown in figure 8 the problem has been approached by steps: first of all, heat equation was solved, then all stresses inducted by thermal expansion and variation in the temperature given by internal stresses. Finally, the phase changing was integrated in the thermo-mechanical coupling.

In order to consider the time evolution, the finite differences method has been applied, so that the $f(\dot{t}) \approx \frac{f(t+\Delta t)-f(t)}{\Delta t}$

Where:

• f is one of the functions needed, which depends on time;

• Δt is the time step;

• t is the time instant.

For the first step the resolution of the heat equation is needed.

$$\rho c_P \dot{T} - div\left(\lambda \cdot \overrightarrow{grad}\, T\right) - q = 0 \quad (3.1)$$

To solve Heat equation with Finite Elements, we will use Galerkin's method of weighted residuals by which Heat equation is multiplied by an arbitrary function T^* called virtual temperature field and integrated over the volume V to obtain $\mathcal{W}(T, T^*)$

The integration is made with four Gauss points as follows:

$$\iiint f(x,y,z)dxdydz = e \iint f(x,y)dxdy$$

With e thickness for the 2D model.

$$\iint f(x,y)dxdy = \iint det\, J(\xi,\eta)\, f(\xi,\eta)d\xi d\eta$$

With J Jacobian matrix. So:

$$\iint det\, J(\xi,\eta)\, f(\xi,\eta)d\xi d\eta = \sum_{i=1}^{4}\sum_{i=1}^{4} {\omega_i}^2\, det\, J(\xi_i,\eta_i)\, f(\xi_i,\eta_i)$$

With: $\omega_i = [1,1,1,1]$

$$\xi_i = \left\{-\sqrt{1/3}, -\sqrt{1/3}, \sqrt{1/3}, \sqrt{1/3}\right\}$$

$$\eta_i = \left\{-\sqrt{1/3}, \sqrt{1/3}, -\sqrt{1/3}, \sqrt{1/3}\right\}$$

In the case of discretization of the temperature with weak integral form we have:

$$[C]\{\dot{T}\} + [K]\{T\} - \{F\} = 0 \quad (3.2)$$

[C] is the thermic rigidity matrix (J/K);

[K] is the thermal conductivity matrix (W/K);

{F} is the vector of nodal fluxes (W);

{T} is the vector of nodal temperatures (K).

The integral form of these matrices is:

$$[C] = \int_V \rho c_p [N]^T [N] dV$$

$$[K] = \int_V [B]^T \lambda [B] dV$$

$$\{F\} = \int_V [N]^T q\, dV = \{0\}$$

Because $q = 0$ as we have applied limit condition just imposing a temperature and so nodal fluxes are constantly

zero. By considering the time evolution, we used the following finite differences equation:

$$\{T\}^{j+1} = \frac{1}{\Delta t}\left[\tilde{K}\right]^{-1}[C]\{T\}^{j} \qquad (3.3)$$

Where: $\left[\tilde{K}\right] = \frac{[C]}{\Delta t} + [K]$

For the other steps the equations 2.3, 2.5 and 2.6 were used with the same approach.

3.2 Mounting pressure

As far as the initial condition are concerned, it has been considered that to mount the disk over the pipe, a mechanical cycle is firstly executed. In our modelling, the clamping pressure has a value of p_{int}=0,85MPa, which is not enough to offer a leak free joint. The cycle for stress calculation will start from this value of pressure, which will be applied to all the nodes at the inner diameter.

3.3 Air Modelling

To impose a realistic heating cycle to the ring, a source with a constant thermal flux have been supposed. The procedure consisted in modelling the air around the disk, as still and not movable. To impose a realistic heating cycle to the ring, a source with a constant thermal flux have been supposed. The procedure consisted in modelling the air around the disk, as still and not movable. Subsequently, a fixed temperature has been imposed at the outer diameter (T_∞) which triggers the variation of the temperature at each node for each time step. Finally, the temperature at the outer diameter of the ring is considered reduced by an η coefficient (η=0,89) with respect to the air temperature. This coefficient can be considered as an efficiency for the heat exchange, due to the convection effect not considered in the model.

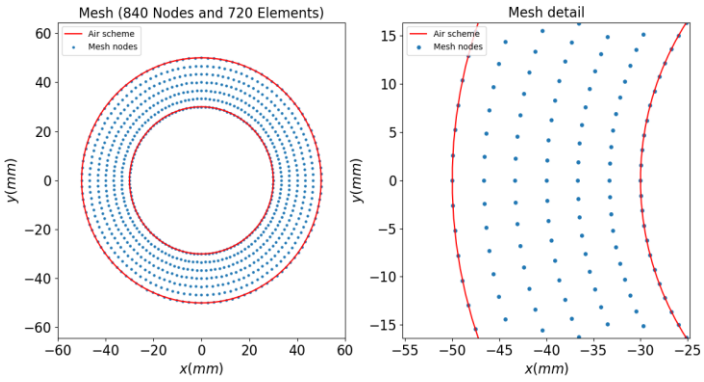

a.

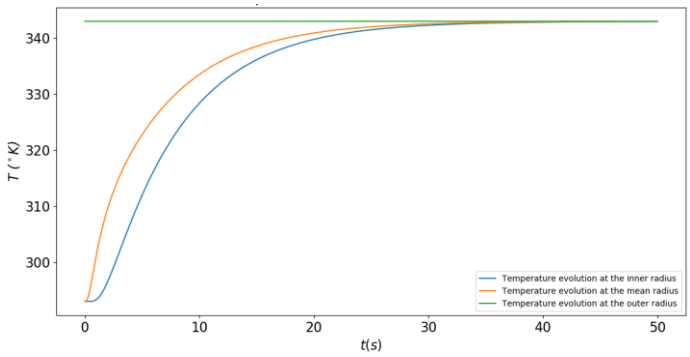

b.

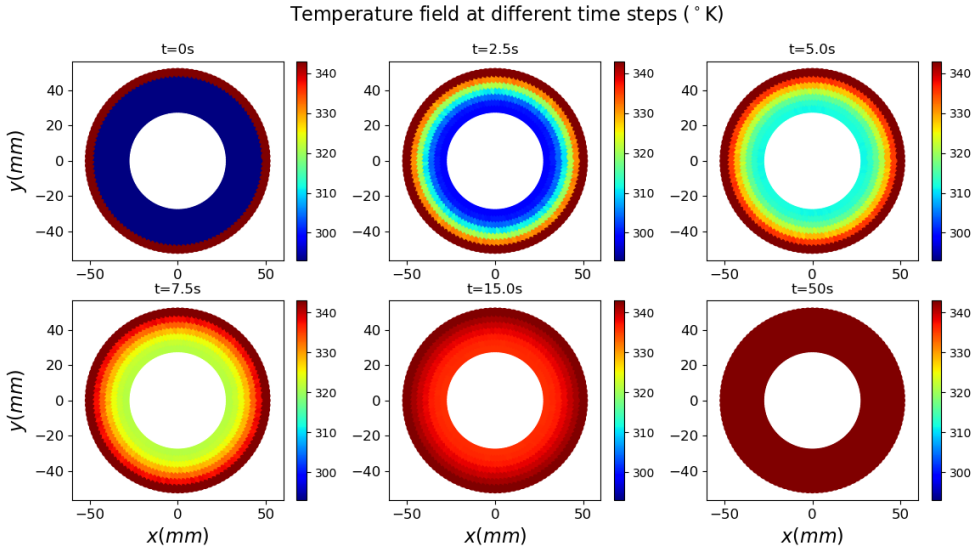

c.

Figure 10- a: Air mesh visualisation (left) and detali (right)l, b: Temperature evolution of air for different time steps at inner, mean and outer radius, c: Temperature field at different time steps

3.4 Ring Modelling

When modelling the ring the assumption of planar stresses has been made. Hence it was possible to conceive a 2D model with planar squared elements. This strong hypothesis is yet acceptable because of the axial symmetry of the model. The 1D model, in fact, allows an economization in terms of processing time of calculus.

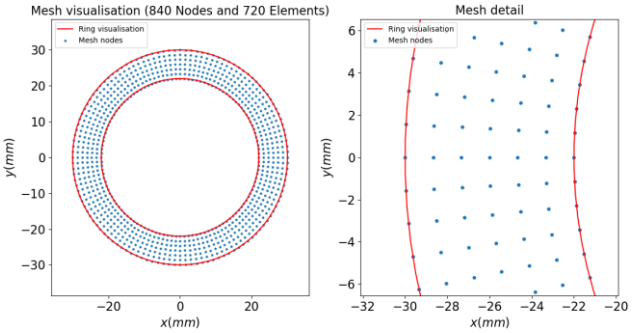

a.

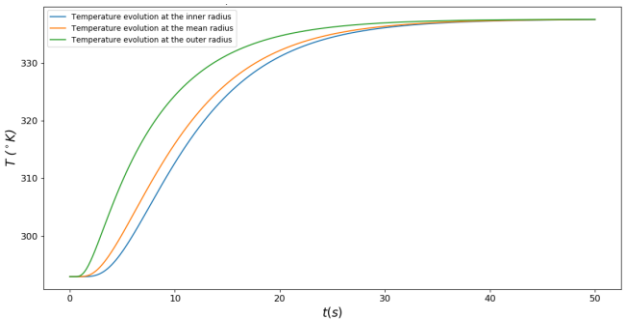

b.

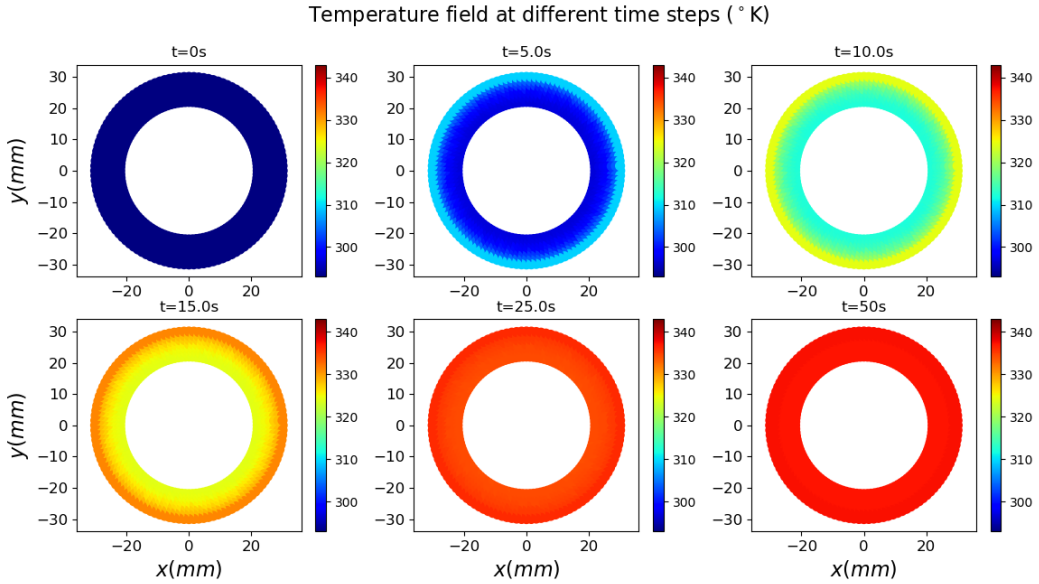

c.

Figure 11- a: Ring mesh visualisation (left) and detil (right)l, b: Temperature evolution of air for different time steps at inner, mean and outer radius, c: Temperature field at different time steps

4. Results

The results of the simulation will be illustrated step by step.

In the first graph (figure 12) it is possible to analyze the results of the first simulation, correlated to the heating cycle: the middle curve shows the evolution of the temperature in the ring during time and in the curve below it is possible to appreciate the speed of variation of the latter. Consequently it is possible to assess that the main phenomena due to thermal effect are concentrated in the first instants. Actually after 15 seconds the transient behaviour arrives to a stabilisation as the temperature curve reaches a plateau.

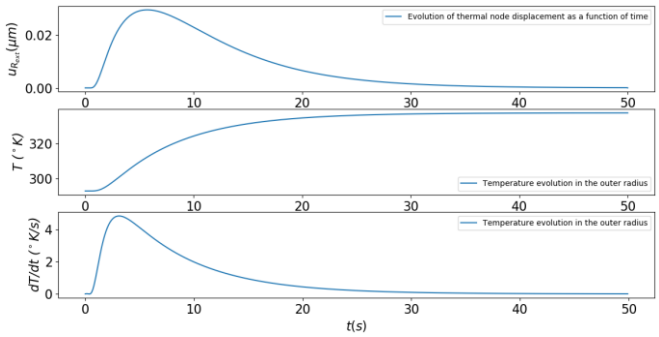

Figure 12-Evolution of node displacement (top), temperature (middle), variation of temperature (bottom) as a function of time

Once analysed the thermal effects, the weak thermomechanical coupling was simulated, taking into account the stresses induced by the heating cycle. As it can be seen in figure 15, the maximum value of the stress reached in this case is around 20 MPa. Subsequently the strong coupling was added, concerning the change in temperature due to the induced stresses. In this case the value of the stress doubles, reaching up to 40 MPa in the inner radius. As it is possible to observe in figure 14 the strain doubles when doubling the stresses, as it passes from 0.05% for a weak coupling to a 0.1% for a strong thermomechanical coupling. This emphasizes the direct proportionality between σ and ε.

Lastly the phase transformation was simulated. The results of the simulation are shown in figure 16. In this case, a sharp increase in both strain and stresses can be appreciated. This is due to the phase change triggered by the temperature increase in a given zone. The phase transformation induces, at microscopic scale, a distortion in the crystalline lattice, which, at a macroscopic scale, is translated in a strain, assumed in the simulation of the 0.1%. With the phase change, internal stresses of 300 MPa are reached, which are, to any extent, still in the elastic strain field.

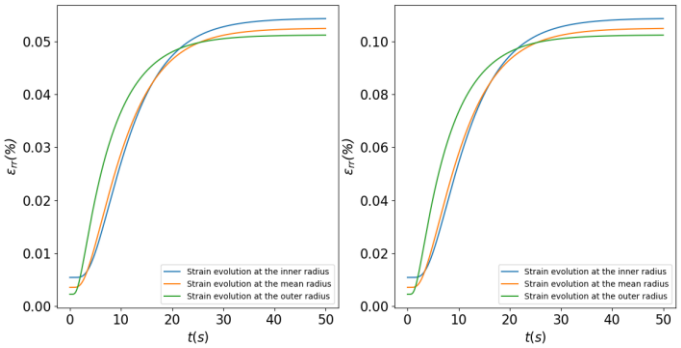

Figure 13-Strain variation for a weak (left) and a strong (right) thermomechanical coupling

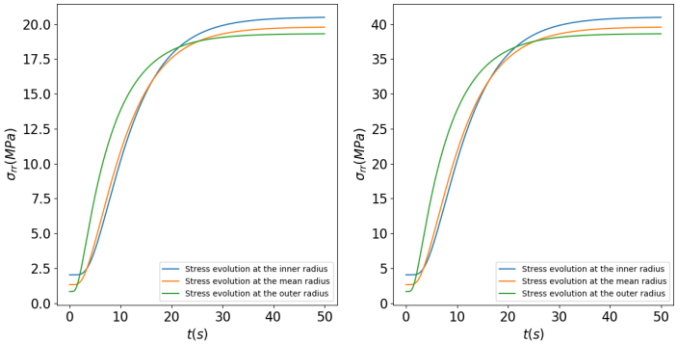

Figure 14- Stress variation for a weak (left) and a strong (right) thermomechanical coupling

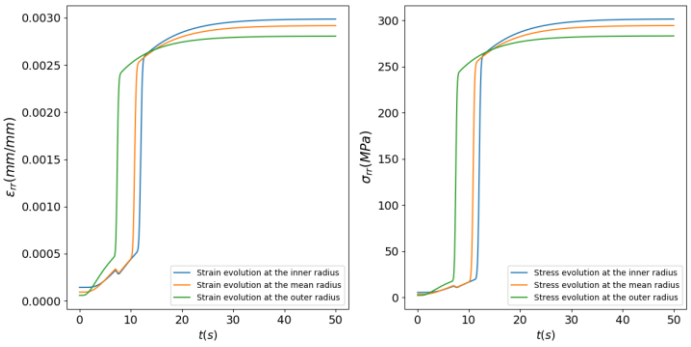

Figure 15- Strain (left) and stress variation for a strong thermomechanical coupling with phase transformation

6. Conclusions

The objective of this work was to prove that with an SMA ring it is possible to create a leak tight joint between two pipes. The real advantage of this system is that it can be used with different materials, it can be actuated remotely (which is of massive importance in radioactive areas) and it can be easily mounted and dismounted without damaging the material of the pipe [1]. The results found have confirmed all these characteristics.

It is, although, important to underline all the different hypothesis made when modelling the system: first of all, a planar stress state has been considered; also, a 1D model was used at the end as all the loads involved have been consider axial symmetrical. Another main hypothesis was taking the value of the strain due to the phase change as the 0.1%. This was issued by considering that, during this kind of process, it is difficult to reach a complete transformation of the lattice. Another assumption made for the sake of simplicity was that the inner radius of the ring has been considered still, already submitted to a mounting pression, which is a non-realistic assumption, as it is the phase change that assures the junction.

In any case the results are appreciable even with all these premises. As it is possible to notice form the graphs the material undergoes a massive increase in the stresses when the phase change is triggered by the increase in temperature. Furthermore, the strong thermo-mechanical coupling is already tensioning the material enough to guarantee a proper seal of the ring.

Acknowledgements

First, we would like to thank Ms. Chiraz Belhadj for giving us the opportunity to develop this project under her supervision during this semester, it has been truly an honour. Thank you for all the advice, ideas, moral support and patience in guiding us through this project. We would also thank Mr. Naman Recho for his contribution in validating our hypothesis in the finite element calculus. Last but not least, we would like to thank the school EPF of Sceaux, Ms. Marie-Thérèse Auclair and Mr. Cedric Zaccardi, for the wonderful chance to have an international exchange of knowledge and points of view. It has been a truly enriching adventure.

References

[1] Niccoli ,Shape memory alloys (SMAs) for remote connection of beam pipes in radioactive areas, CERN, Università della Calabria

[2] Depriester, Maynadier, Lavernhe-Taillard, Hubert, 2014, Thermomechanical modelling of a NiTi SMA sample submittedto displacement-controlled tensile test, International Journal of Solids and Structures

[3] Niccoli, Shape Memory Alloy connectors for Ultra High Vacuum applications: a breakthrough for accelerator technologies, Università della Calabria

[4] Terriault, Viens, Brailovski, 2006, Non-isothermal finite element modeling of a shape memory alloy actuator using ANSYS, Computational Material Science

[5] Divringi, Ozcan, 2016, Advanced Shape Memory Alloy Material Models for ANSYS, Ozen Engineering